Enhancing $B_s \to e^+e^-$ to an observable level in the two-Higgs-doublet model

Matthew Black,[1,*] Alexis D. Plascencia,[2,†] and Gilberto Tetlalmatzi-Xolocotzi[1,3,‡]

[1]*Theoretische Physik 1, Center for Particle Physics Siegen (CPPS), Universität Siegen, Walter-Flex-Str. 3, 57068 Siegen, Germany*

[2]*INFN, Laboratori Nazionali di Frascati, C.P. 13, 100044 Frascati, Italy*

[3]*Université Paris-Saclay, CNRS/IN2P3, IJCLab, 91405 Orsay, France*

(Received 17 November 2022; accepted 27 January 2023; published 16 February 2023)

As a result of the helicity suppression effect, within the Standard Model the rare decay channel $B_s \to e^+e^-$ has a decay probability that is five orders of magnitude below current experimental limits. Thus, any observation of this channel within the current or forthcoming experiments will give unambiguous evidence of physics beyond the Standard Model. In this work, we present for the first time a new physics scenario in which the branching fraction $\bar{\mathcal{B}}r(B_s \to e^+e^-)$ is enhanced up to values which saturate the current experimental bounds. More concretely, we study the general two-Higgs-doublet model with a pseudoscalar coupling to electrons unsuppressed by the electron mass. Furthermore, we demonstrate how this scenario can arise from a UV-complete theory of quark-lepton unification that can live at a low scale. This latter step allows us to establish correlations between $B_s \to e^+e^-$ and the lepton-flavor-violating decays $\tau^- \to \mu^-e^+e^-$ and $\tau \to \mu\gamma$.

DOI: 10.1103/PhysRevD.107.035013

I. INTRODUCTION

The rare decays $B_s \to \ell^+\ell^-$ for $\ell = e, \mu, \tau$ are characterized by interesting properties that make them quite special and suitable to test the Standard Model (SM) and to search for new physics (NP). For instance within the SM these transitions are only possible as loop-induced processes. Moreover, they are extremely clean since only leptons are present in the final state and all of the nonperturbative hadronic effects are contained in the decay constant of the initial B_s meson. As a matter of fact the B meson decay constants are currently known with a precision of less than 1% [1–5].

One of the particular features of the B_s meson rare processes is that their decay probability in the SM is proportional to the mass of the final state lepton; this is the so-called helicity suppression effect. For muons in the final state, this leads to a SM branching fraction of $\bar{\mathcal{B}}r(B_s \to \mu^+\mu^-) = (3.55 \pm 0.10) \times 10^{-9}$ that, in spite of being already quite small, has being measured by different experimental collaborations leading to a combined result which is in good agreement with the theoretical determination [6–9].

Due to the tiny mass of the electrons, for the channel $B_s \to e^+e^-$ the helicity suppression is maximal. Indeed, in the SM we have $\bar{\mathcal{B}}r(B_s \to e^+e^-) = (8.30 \pm 0.36) \times 10^{-14}$, which is about four orders of magnitude below the corresponding value for $B_s \to \mu^+\mu^-$. Consequently, for a long time the experimental search for this channel was not pursued. As a matter of fact, until 2020 the only experimental result available was the upper bound reported by the CDF collaboration [10], which was then updated by the LHCb experiment [11] with the result

$$\bar{\mathcal{B}}r(B_s \to e^+e^-) < 9.4 \times 10^{-9}. \tag{1.1}$$

Due to the large difference between the most recent experimental bounds on $\bar{\mathcal{B}}r(B_s \to e^+e^-)$ and the corresponding SM prediction we can conclude that any observation of this channel in the foreseeable future can only be a manifestation of physics beyond the SM. Following a model-independent approach, in [12] it was shown how the presence of NP pseudoscalar interactions could enhance the SM decay probability up to values which can potentially saturate the known experimental bounds. One of the main requirements to achieve this effect is that the NP couplings should not be proportional to the mass of the electron m_e. This then excludes models where the coupling between the NP pseudoscalars and the final state electrons is determined at leading order by the mass m_e.

*matthew.black@uni-siegen.de
†alexis.plascencia@lnf.infn.it
‡gtx@physik.uni-siegen.de

In this work, we present a minimal extension of the SM based on the type-III two-Higgs-doublet model (2HDM), in which a second Higgs is introduced with the same quantum numbers as the SM Higgs and both scalar doublets are coupled to quarks and leptons. We show how this scenario gives enough freedom to obtain couplings between the electrons and the relevant scalar and pseudoscalar particles that allow us to achieve large enhancements on $\bar{\mathcal{B}}r(B_s \to e^+e^-)$ while obeying all the relevant phenomenological constraints. The literature on 2HDM is vast, for reviews on the topic we refer the reader to Refs. [13,14].

Furthermore, we study how the type-III 2HDM scenario with the properties outlined above can arise from a UV theory of quark-lepton unification. J. Pati and A. Salam [15] postulated the idea of matter unification in which the SM quarks and leptons belong to the same multiplet and this approach remains as one of the best-motivated frameworks for physics beyond the SM. However, since the top quark Yukawa coupling is predicted to be the same as the Dirac neutrino coupling, then the seesaw mechanism [16–19] requires the energy scale associated with the theory to be very high $\sim 10^{14}$ GeV, making it hard to be phenomenologically tested. Consequently, here we consider the theory proposed in Ref. [20], which can be regarded as a low energy limit of the original Pati-Salam scenario, in which neutrinos acquire their mass through the inverse seesaw mechanism [21,22] and the theory can be realized at a low energy scale.

This paper is structured as follows. In Sec. II, we overview the experimental and theoretical status regarding the B_s meson rare decays. In Sec. III, we discuss the general 2HDM and study the Wilson operators generated in this model. In Sec. IV, we present the corresponding predictions for $\bar{\mathcal{B}}r(B_s \to e^+e^-)$ and study the phenomenological constraints on the parameter space considering different observables. In Sec. V, we present the theoretical motivation from a theory of quark-lepton unification. Finally, our conclusions are presented in Sec. VI.

II. B_s MESON RARE DECAYS

In order to address the decays $B_s \to \ell^+\ell^-$ we consider the following effective Hamiltonian

$$\mathcal{H}_{\text{eff}} = -\frac{G_F V_{tb} V_{ts}^* \alpha}{\sqrt{2}\pi}[C_{10}^{\ell\ell} O_{10}^{\ell\ell} + C_S^{\ell\ell} O_S^{\ell\ell} + C_P^{\ell\ell} O_P^{\ell\ell} + C_{10'}^{\ell\ell} O_{10'}^{\ell\ell} + C_{S'}^{\ell\ell} O_{S'}^{\ell\ell} + C_{P'}^{\ell\ell} O_{P'}^{\ell\ell}] + \text{H.c.}, \tag{2.1}$$

where

$$\begin{aligned} \mathcal{O}_{10}^{\ell\ell} &= (\bar{s}\gamma_\mu P_L b)(\bar{\ell}\gamma^\mu\gamma_5\ell), & \mathcal{O}_{10'}^{\ell\ell} &= (\bar{s}\gamma_\mu P_R b)(\bar{\ell}\gamma^\mu\gamma_5\ell), \\ \mathcal{O}_S^{\ell\ell} &= m_b(\bar{s}P_R b)(\bar{\ell}\ell), & \mathcal{O}_{S'}^{\ell\ell} &= m_b(\bar{s}P_L b)(\bar{\ell}\ell), \\ \mathcal{O}_P^{\ell\ell} &= m_b(\bar{s}P_R b)(\bar{\ell}\gamma^5\ell), & \mathcal{O}_{P'}^{\ell\ell} &= m_b(\bar{s}P_L b)(\bar{\ell}\gamma^5\ell), \end{aligned} \tag{2.2}$$

for $\ell = e, \mu, \tau$.

The description of the B_s meson rare decays $B_s \to \ell^+\ell^-$ is given in terms of two measurable quantities that offer complementary information. The first one is the time-integrated branching fraction [12,23]

$$\bar{\mathcal{B}}r(B_s \to \ell^+\ell^-) = \frac{1}{2}\int_0^\infty \langle \Gamma(B_s(t) \to \ell^+\ell^-)\rangle dt, \tag{2.3}$$

and the second one is the effective lifetime

$$\tau_{\ell\ell} \equiv \frac{\int_0^\infty t\langle \Gamma(B_s(t) \to \ell^+\ell^-)\rangle dt}{\int_0^\infty \langle \Gamma(B_s(t) \to \ell^+\ell^-)\rangle dt}, \tag{2.4}$$

which is equivalent to the observable

$$\mathcal{A}_{\Delta\Gamma_s}^{\ell\ell} = \frac{1}{y_s}\frac{(1-y_s^2)\tau_{\ell\ell} - (1+y_s^2)\tau_{B_s}}{2\tau_{B_s} - (1-y_s^2)\tau_{\ell\ell}}. \tag{2.5}$$

In Eq. (2.5), τ_{B_s} refers to the lifetime of the B_s meson. In addition, the neutral B_s mixing effects are accounted for by

$$y_s \equiv \frac{\Delta\Gamma_s}{2\Gamma_s}, \tag{2.6}$$

where $\Delta\Gamma_s$ is the decay width difference between the B_s and $\bar{B}_s$ mesons. Moreover, the untagged rate is defined as

$$\begin{aligned} \langle \Gamma(B_s(t) \to \ell^+\ell^-)\rangle &\equiv \Gamma(B_s^0(t) \to \ell^+\ell^-) + \Gamma(\bar{B}_s^0(t) \to \ell^+\ell^-), \\ &= \Gamma(B_s \to \ell^+\ell^-)_{\text{prompt}} \times e^{-t/\tau_{B_s}}(\cosh(y_s t/\tau_{B_s}) + \mathcal{A}_{\Delta\Gamma_s}^{\ell\ell}\sinh(y_s t/\tau_{B_s})), \end{aligned} \tag{2.7}$$

where

$$\Gamma(B_s \to \ell^+\ell^-)_{\text{prompt}} = \frac{G_F^2\alpha^2}{16\pi^3}|V_{ts}V_{tb}^*|^2 f_{B_s}^2 M_{B_s} m_\ell^2\sqrt{1-4\frac{m_\ell^2}{M_{B_s}^2}}|C_{10}^{\text{SM}}|^2(|P_{\ell\ell}|^2 + |S_{\ell\ell}|^2). \tag{2.8}$$

The functions $P_{\ell\ell}$ and $S_{\ell\ell}$ are given by

$$P_{\ell\ell} \equiv \frac{C_{10}^{\ell\ell} - C_{10'}^{\ell\ell}}{C_{10}^{\mathrm{SM}}} + \frac{M_{B_s}^2}{2m_\ell}\left(\frac{m_b}{m_b+m_s}\right)\left[\frac{C_P^{\ell\ell} - C_{P'}^{\ell\ell}}{C_{10}^{\mathrm{SM}}}\right],$$
$$S_{\ell\ell} \equiv \sqrt{1-4\frac{m_\ell^2}{M_{B_s}^2}}\frac{M_{B_s}^2}{2m_\ell}\left(\frac{m_b}{m_b+m_s}\right)\left[\frac{C_S^{\ell\ell} - C_{S'}^{\ell\ell}}{C_{10}^{\mathrm{SM}}}\right]. \quad (2.9)$$

In the SM, $C_P^{\ell\ell} = C_{P'}^{\ell\ell} = C_S^{\ell\ell} = C_{S'}^{\ell\ell} = 0$, leading to

$$P_{\ell\ell}^{\mathrm{SM}} = 1, \qquad S_{\ell\ell}^{\mathrm{SM}} = 0, \quad (2.10)$$

thus the branching fraction simplifies to

$$\bar{\mathcal{B}}r(B_s \to \ell^+\ell^-)_{\mathrm{SM}} = \frac{1}{1-y_s}\frac{G_F^2\alpha^2}{16\pi^3}\tau_{B_s}|V_{ts}V_{tb}^*|^2 f_{B_s}^2 M_{B_s} m_\ell^2 \times \sqrt{1-4\frac{m_\ell^2}{M_{B_s}^2}}|C_{10}^{\mathrm{SM}}|^2. \quad (2.11)$$

For real Wilson coefficients, the theoretical branching fraction for the process $B_s \to \ell^+\ell^-$ is

$$\bar{\mathcal{B}}r(B_s \to \ell^+\ell^-) = \bar{\mathcal{B}}r(B_s \to \ell^+\ell^-)_{\mathrm{SM}} \times \left[|P_{\ell\ell}|^2 + \frac{1-y_s}{1+y_s}|S_{\ell\ell}|^2\right]. \quad (2.12)$$

An analogous expression in terms of $P_{\ell\ell}$ and $S_{\ell\ell}$ can also be written for $\tau_{\ell\ell}$. However, due to the equivalence with $\mathcal{A}_{\Delta\Gamma_s}^{\ell\ell}$ we only provide an explicit expression for the latter:

$$\mathcal{A}_{\Delta\Gamma_s}^{\ell\ell} = \frac{|P_{\ell\ell}|^2 - |S_{\ell\ell}|^2}{|P_{\ell\ell}|^2 + |S_{\ell\ell}|^2}, \quad (2.13)$$

and finally, $\tau_{\ell\ell}$ can be obtained by applying Eq. (2.5).

As can be seen in Eq. (2.11), in the SM, the decay probability $\bar{\mathcal{B}}r(B_s \to \ell^+\ell^-)_{\mathrm{SM}}$ is proportional to the square of the mass of the final state lepton m_ℓ^2. Since muons and electrons are particularly light, for $\bar{\mathcal{B}}r(B_s \to \mu^+\mu^-)_{\mathrm{SM}}$ and $\bar{\mathcal{B}}r(B_s \to e^+e^-)_{\mathrm{SM}}$ the masses m_μ and m_e, respectively, act as suppression factors. Then the SM predictions for the branching fractions for the different rare decays are

$$\bar{\mathcal{B}}r(B_s \to e^+e^-)_{\mathrm{SM}} = (8.30 \pm 0.22) \times 10^{-14}, \quad (2.14)$$

$$\bar{\mathcal{B}}r(B_s \to \mu^+\mu^-)_{\mathrm{SM}} = (3.55 \pm 0.10) \times 10^{-9}, \quad (2.15)$$

$$\bar{\mathcal{B}}r(B_s \to \tau^+\tau^-)_{\mathrm{SM}} = (7.52 \pm 0.20) \times 10^{-7}. \quad (2.16)$$

For the experimental value of $\bar{\mathcal{B}}r(B_s \to \mu^+\mu^-)$ we update the result presented in [24] by performing a weighted average including the measurements from LHCb, ATLAS, and the latest value from CMS [6–9]:

$$\bar{\mathcal{B}}r(B_s \to \mu^+\mu^-)_{\mathrm{Exp}} = (3.39 \pm 0.29) \times 10^{-9}. \quad (2.17)$$

In addition, LHCb has performed two pioneering measurements of the effective lifetime $\tau_{\mu\mu}$ [6,7,25]. Combining [7,9] we obtain

$$\tau_{\mu\mu} = 1.83 \pm 0.21 \text{ ps}. \quad (2.18)$$

For examples of studies on $B_s \to \mu^+\mu^-$ and more generically on $b \to s\ell^+\ell^-$ processes within the context of 2HDM see for example [26,27].

In the case of $B_s \to \tau^+\tau^-$ the current 95% C.L. bound is available [28]:

$$\bar{\mathcal{B}}r(B_s \to \tau^+\tau^-) < 6.8 \times 10^{-3}. \quad (2.19)$$

Notice that according to Eq. (2.16), in the SM the decay ratio $\bar{\mathcal{B}}r(B_s \to \tau^+\tau^-)$ has the largest value amongst all final state leptons, however the reconstruction of the τ particle is a challenging task, making the experimental extraction of the corresponding decay ratio especially difficult.

Finally, due to the tiny mass of the electron, the transition $B_s \to e^+e^-$ is rather suppressed in the SM. Indeed, as can be seen in Eq. (2.14), this channel has the lowest branching fraction among all the possible leptonic final states and lies outside the reach of current or future particle physics experiments. However, the presence of NP scalar and pseudoscalar mediators can drastically enhance the value of $\bar{\mathcal{B}}r(B_s \to e^+e^-)$ [12]. As shown in Eq. (2.9), this effects boils down to the presence of the tiny factor $m_\ell = m_e$ in the denominators of the functions $P_{\ell\ell} = P_{ee}$ and $S_{\ell\ell} = S_{ee}$, which for nonzero contributions of the differences $\Delta C_P^{\ell\ell} = C_P^{\ell\ell} - C_{P'}^{\ell\ell}$ and $\Delta C_S^{\ell\ell} = C_S^{\ell\ell} - C_{S'}^{\ell\ell}$ can maximally lift the helicity suppression induced in the SM. In this respect, the decay channel $B_s \to e^+e^-$ is special since its measurement in any foreseeable experimental facility will be a clear and unambiguous indication of NP.

In 2009, CDF reported the first bound on the production rate of this particular channel at 90% C.L.:

$$\bar{\mathcal{B}}r(B_s \to e^+e^-)_{\mathrm{Exp,CDF}} < 2.8 \times 10^{-7}. \quad (2.20)$$

This bound was updated recently by the LHCb collaboration [11] leading to the following 90(95)% C.L. bounds:

$$\bar{\mathcal{B}}r(B_s \to e^+e^-)_{\mathrm{Exp,LHCb}} < 9.4(11.2) \times 10^{-9}. \quad (2.21)$$

As described previously, the potential enhancement on $\bar{\mathcal{B}}r(B_s \to e^+e^-)$ as the result of NP scalar and pseudoscalar particles was first noticed in [12] in a model-independent fashion. To the best of our knowledge an analysis within the context of a renormalizable NP framework has not been

performed so far. In the following sections we take this next step and develop a NP scenario where this effect can arise.

In order to perform the numerical calculations corresponding to the B-physics processes, in this work we will make use of the flavor physics package FLAVIO[1] [29]. This will also allow us to combine observables in frequentist likelihood fits of experimental data to determine constraints on the parameters of our NP model. FLAVIO describes NP contributions model independently using effective field theories (EFTs) where NP enters as additions to the Wilson coefficients of the operators of the EFT. Of interest here is the weak effective theory with five active flavors (defined at the scale m_b), where we can directly describe the contributions from our model in the language of the relevant Wilson coefficients as laid out below.

III. THE GENERAL 2HDM AND THE PROCESS $B_s \to e^+e^-$

In this section, we will focus on a mechanism that lifts the helicity suppression in $\bar{\mathcal{B}}r(B_s \to e^+e^-)$ leading to a large enhancement within a minimal extension of the SM. Namely, extending the SM with a second Higgs doublet with the same quantum numbers as the SM one; for reviews on the 2HDM we refer the reader to Refs. [13,14]. In the general 2HDM, both Higgs doublets are coupled to the quarks and leptons; this scenario is commonly referred to in the literature as the type-III 2HDM. Therefore, we can write the following Yukawa interactions,

$$-\mathcal{L} \supset \bar{Q}_L(Y_1^u\tilde{H}_1 + Y_2^u\tilde{H}_2)u_R + \bar{Q}_L(Y_1^dH_1 + Y_2^dH_2)d_R + \bar{\ell}_L(Y_1^eH_1 + Y_2^eH_2)e_R + \text{H.c.}, \tag{3.1}$$

with $H_1^T = (H_1^+, (v_1 + H_1^0 + iA_1^0)/\sqrt{2})$, $\tilde{H}_1 = i\sigma_2 H_1^*$ and correspondingly for H_2. The vacuum expectation values (VEVs) are defined by $\langle H_1^0\rangle = v_1$ and $\langle H_2^0\rangle = v_2$.

The scalar potential for H_1 and H_2 with quantum numbers $(\mathbf{1},\mathbf{2},1/2)$ corresponds to

$$\begin{aligned} V(H_1,H_2) = {} & m_{11}^2H_1^\dagger H_1 + m_{22}^2H_2^\dagger H_2 - m_{12}^2[(H_1^\dagger H_2) + \text{H.c.}] \\ & + \frac{\lambda_1}{2}(H_1^\dagger H_1)^2 + \frac{\lambda_2}{2}(H_2^\dagger H_2)^2 + \lambda_3(H_1^\dagger H_1)(H_2^\dagger H_2) + \lambda_4(H_1^\dagger H_2)(H_2^\dagger H_1) \\ & + \left[\frac{\lambda_5}{2}(H_1^\dagger H_2)^2 + \lambda_6(H_1^\dagger H_1)(H_1^\dagger H_2) + \lambda_7(H_2^\dagger H_2)(H_1^\dagger H_2) + \text{H.c.}\right]. \end{aligned} \tag{3.2}$$

The physical Higgs fields are defined by

$$\begin{pmatrix} H \\ h \end{pmatrix} = \begin{pmatrix} \cos\alpha & \sin\alpha \\ -\sin\alpha & \cos\alpha \end{pmatrix}\begin{pmatrix} H_1^0 \\ H_2^0 \end{pmatrix}, \tag{3.3}$$

$$\begin{pmatrix} G \\ A \end{pmatrix} = \begin{pmatrix} \cos\beta & \sin\beta \\ -\sin\beta & \cos\beta \end{pmatrix}\begin{pmatrix} A_1^0 \\ A_2^0 \end{pmatrix}, \tag{3.4}$$

$$\begin{pmatrix} G^\pm \\ H^\pm \end{pmatrix} = \begin{pmatrix} \cos\beta & \sin\beta \\ -\sin\beta & \cos\beta \end{pmatrix}\begin{pmatrix} H_1^\pm \\ H_2^\pm \end{pmatrix}, \tag{3.5}$$

where h is identified as the SM-like Higgs and H as an additional neutral Higgs. In addition, $H_i^0, H_i^\pm, A_i^0$ are the neutral, charged and CP-odd components of the Higgs doublets respectively. Finally $G, G^\pm$ are the wouldbe Goldstone bosons. The mixing angle β is defined by the ratio of the VEVs of the Higgs doublets, $\tan\beta = v_2/v_1$ and we use $v^2 = v_1^2 + v_2^2$. The couplings of h are SM-like in the alignment limit $\sin(\beta-\alpha) \to 1$, which corresponds to $\alpha = \beta - \pi/2$. Thus, the interactions between the fermions and the neutral scalars can be written as

$$-\mathcal{L} \supset \bar{f}_L^i\left[\frac{M^i_{\text{diag}}}{v}h + \left(-\cot\beta\frac{M^i_{\text{diag}}}{v} + \frac{\Omega^i}{\sqrt{2}s_\beta}\right)(H \pm iA)\right]f_R^i + \text{H.c.}, \tag{3.6}$$

where the super index i denotes the fermion flavor for $i = u, d, e$. In the equation above, the positive sign is assigned to the field A when considering couplings to the up-type quarks while the negative sign is considered for couplings to the down-type quarks and charged leptons. The mass matrices are given by

$$m^i = Y_1^i\frac{v_1}{\sqrt{2}} + Y_2^i\frac{v_2}{\sqrt{2}}, \tag{3.7}$$

and M^i_{diag} in Eq. (3.6) correspond to the diagonal mass matrices $M^i_{\text{diag}} = V_L^{i\dagger}m^iV_R^i$ with unitary V_L^i and V_R^i. Finally, the matrices Ω^i are given by $\Omega^i = V_L^{i\dagger}Y_1^iV_R^i$ and are characterized by general components. We have assumed that all new parameters are real, and hence, that H and A do not mix.

[1] https://flav-io.github.io/.

For the charged leptons we assume the interaction with the heavy Higgs bosons to be very close to flavor diagonal:

$$\tilde{Y}^{\ell} = -\cot\beta \frac{M^E_{\rm diag}}{v} + \frac{\Omega^{\ell}}{\sqrt{2}s_\beta} = \begin{pmatrix} y_{ee} & \varepsilon & \varepsilon \\ \varepsilon & y_{\mu\mu} & \varepsilon \\ \varepsilon & \varepsilon & y_{\tau\tau} \end{pmatrix}, \quad (3.8)$$

where $\varepsilon \ll y_{jj}$. This allows us to evade the strong experimental constraints from the nonobservation of processes which violate lepton flavor such as $\mu \to e\gamma$ [30], $\mu - e$ conversion [31], and $\mu \to eee$ [32]. Since we are mostly interested in the coupling to electrons, we assume the hierarchy $y_{\mu\mu} \ll y_{ee}$ and $\varepsilon \ll y_{\tau\tau}$. As we will discuss in Sec. V, the texture in Eq. (3.8) obeying the indicated hierarchy can be motivated by embedding the 2HDM in a low-energy limit of Pati-Salam unification.

Similarly for the down-type quarks, we assume the Yukawa interaction to be close to the flavor diagonal:

$$\tilde{Y}^{d} = -\cot\beta \frac{M^D_{\rm diag}}{v} + \frac{\Omega^{d}}{\sqrt{2}s_\beta} = \begin{pmatrix} y_{dd} & \varepsilon & \varepsilon \\ \varepsilon & y_{ss} & y_{bs}/2 \\ \varepsilon & y_{bs}/2 & y_{bb} \end{pmatrix}, \quad (3.9)$$

where we write ε for very small numbers obeying $\varepsilon \ll y_{ij}$. Here, we have suppressed some off-diagonal entries in order to avoid the strong bounds coming from measurements of neutral kaon mixing. Also, we have kept the off-diagonal entry y_{bs} since this coupling mediates the process $B_s \to e^+e^-$ at tree level by coupling the NP scalar H and pseudoscalar A to the quarks b and s. Moreover, we have assumed that $\tilde{Y}^d_{sb} = \tilde{Y}^d_{bs} = y_{bs}/2$, a choice that will be motivated in Sec. V. As we shall see below, the experimental constraint from B_s meson mixing requires this coupling to be very small.

The relevant Yukawa interactions affecting the process $B_s \to e^+e^-$ at tree level are

$$-\mathcal{L} \supset y_{ee}\bar{e}eH + y_{bs}\bar{b}sH - iy_{ee}\bar{e}\gamma^5 eA - iy_{bs}\bar{b}\gamma^5 sA, \quad (3.10)$$

where the assumption of no new sources of CP violation implies all couplings and, hence, that H and A do not mix. The expression in Eq. (3.10) will play a central role in our subsequent discussion.

By integrating out the particles A and H inside Eq. (3.10) we can immediately determine the Wilson coefficients $C^{ee}_{S^{(\prime)}}$ and $C^{ee}_{P^{(\prime)}}$ given in Eq. (2.1) in terms of the parameters of our model:

$$C^{ee}_S = \frac{y_{ee}y_{bs}}{M_H^2}\left(\frac{\sqrt{2}\pi}{m_b G_F V_{tb}V^*_{ts}\alpha}\right), \qquad C^{ee}_{S'} = C^{ee}_S, \quad (3.11)$$

$$C^{ee}_P = -\frac{y_{ee}y_{bs}}{M_A^2}\left(\frac{\sqrt{2}\pi}{m_b G_F V_{tb}V^*_{ts}\alpha}\right), \quad C^{ee}_{P'} = -C^{ee}_P, \quad (3.12)$$

where M_H and M_A are the masses of H and A, respectively.

Given that, according to Eqs. (2.8) and (2.9), the branching fraction depends only on the difference $\Delta C^{ee}_S = C^{ee}_S - C^{ee}_{S'}$ and that based on Eq. (3.11) within our model $C^{ee}_S = C^{ee}_{S'}$, we can immediately see that the CP-even scalar H does not contribute to the observable $\bar{\mathcal{B}}r(B_s \to e^+e^-)$. However, the CP-odd scalar (pseudoscalar) A can have large effects. A crucial point to highlight is that in our NP scenario, the coupling between the heavy Higgs bosons and electrons is not required to be proportional to the mass of the electron; this is of capital importance when lifting the SM helicity suppression.

The values of the masses M_H and M_A depend on the parameters of the 2HDM scalar potential $\lambda_{1\to 7}, m^2_{12}$, $\tan\beta$ and α [see Eq. (3.2)] [33]. Hence M_H and M_A are not independent from each other and are actually correlated. The parameters in the scalar potential are constrained by different theoretical conditions such as perturbativity and vacuum stability that can be combined as follows [33]:

$$0 < \lambda_{1,2} < 4, \quad (3.13)$$

$$-\sqrt{\lambda_1\lambda_2} < \lambda_3 < 4, \quad (3.14)$$

$$-4 < \lambda_{4,5,6,7} < 4. \quad (3.15)$$

Therefore, to determine the allowed values for M_A and M_H, we randomly sample through the parameter space of the scalar potential that in addition delivers the masses of the charged scalars $M_{H^\pm}$. In order to simplify the scan we assume that all the parameters in the scalar potential are real. During this procedure, we use the mass of the SM Higgs boson as a constraint, i.e., we take $M_h = M_h^{\rm SM} = 125.25 \pm 0.17$ GeV [34] as well as the inequality $M_h \le M_H$, and fix $\sin(\beta - \alpha) = 1$.

In Fig. 1 we present our results for the allowed values of M_A and M_H after imposing these constraints on the parameters in the scalar potential. For small masses below 1 TeV, the mass splitting between M_A and M_H can be quite large (around 500 GeV), while for heavy masses around 10 TeV, this difference must be rather small (around 50 GeV), and hence the heavy mass regime satisfies $M_A = M_H$ to a very good approximation. In this limit the NP Wilson coefficients given in Eq. (3.11) satisfy $C^{ee}_P = -C^{ee}_S$ and $C^{ee}_{P'} = C^{ee}_{S'}$, which are two well-known relationships obtained in SMEFT.

IV. ENHANCING $B_s \to e^+e^-$ AND PHENOMENOLOGICAL CONSTRAINTS

Our next task is to determine bounds for the couplings y_{bs} and y_{ee} to quarks and leptons respectively based on the

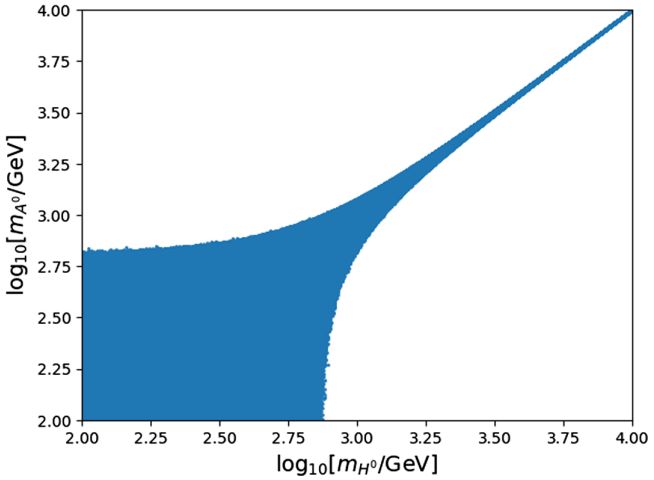

FIG. 1. Correlation between the masses M_A and M_H from the constraints on the 2HDM scalar potential. A total of 10^9 points fulfilling the conditions on the theory were generated in the limit of $\sin(\beta-\alpha)=1$ and defining the perturbativity limits as $|\lambda_i|<4$. The region shaded in blue shows the masses for successful parameters of the 2HDM scalar potential.

phenomenological constraints available. We first focus on the bounds on the y_{ee} coupling from the measurement of the cross section for $e^-e^+\to e^-e^+$ performed by the LEP collaboration. Their reported constraints on the four-electron axial-vector interaction [35] can be translated to the scalar and pseudoscalar interactions; we find that the 95% confidence level lower bound is determined by

$$\frac{y_{ee}^2}{M_H^2}+\frac{y_{ee}^2}{M_A^2}<\frac{1}{(4\ \text{TeV})^2}. \tag{4.1}$$

In the case where $M_H=M_A$, this bound becomes

$$\frac{y_{ee}}{M_H}<\frac{1}{(5.7\ \text{TeV})}. \tag{4.2}$$

The observable ΔM_s is sensitive to the presence of NP scalar and pseudoscalar particles and thus can impose strong constraints on the coupling y_{bs}; the new tree-level diagrams mediated by H and A are shown in Fig. 2. In this work we will consider the following set of $\Delta B=2$ operators that contribute to ΔM_s:

$$\begin{aligned}
\mathcal{O}_V^{\Delta B=2}&=\bar{s}_i\gamma^\mu(1-\gamma_5)b_i\bar{s}_j\gamma_\mu(1-\gamma_5)b_j,\\
\mathcal{O}_{LL}^{\Delta B=2}&=\bar{s}_i(1-\gamma_5)b_i\bar{s}_j(1-\gamma_5)b_j,\\
\mathcal{O}_{RR}^{\Delta B=2}&=\bar{s}_i(1+\gamma_5)b_i\bar{s}_j(1+\gamma_5)b_j,\\
\mathcal{O}_{LR}^{\Delta B=2}&=\bar{s}_i(1-\gamma_5)b_i\bar{s}_j(1+\gamma_5)b_j,
\end{aligned} \tag{4.3}$$

where in the SM only the coefficient of $\mathcal{O}_V^{\Delta B=2}$ is nonzero. In terms of the parameters of our model in Eq. (3.10), the coefficients of the operators $\mathcal{O}_{LL}^{\Delta B=2}$, $\mathcal{O}_{RR}^{\Delta B=2}$ and $\mathcal{O}_{LR}^{\Delta B=2}$ are, respectively,

$$\begin{aligned}
C_{RR}^{\Delta B=2}&=\frac{y_{bs}^2}{4}\left[\frac{1}{m_H^2}-\frac{1}{m_A^2}\right], \qquad C_{RR}^{\Delta B=2}=C_{LL}^{\Delta B=2},\\
C_{LR}^{\Delta B=2}&=\frac{y_{bs}^2}{2}\left[\frac{1}{m_H^2}+\frac{1}{m_A^2}\right].
\end{aligned} \tag{4.4}$$

The relevant matrix elements of the operators in Eq. (4.3) are given by [36]

$$\begin{aligned}
\langle\mathcal{O}_V^{\Delta B=2}\rangle&=\frac{8}{3}M_{B_s}^2f_{B_s}^2B_1(\mu_b),\\
\langle\mathcal{O}_{LL}^{\Delta B=2}\rangle&=M_{B_s}^2f_{B_s}^2\frac{-5M_{B_s}^2}{3(\bar{m}_b(\mu_b)+\bar{m}_s(\mu_b))^2}B_2(\mu_b),\\
\langle\mathcal{O}_{LL}^{\Delta B=2}\rangle&=\langle\mathcal{O}_{RR}^{\Delta B=2}\rangle,\\
\langle\mathcal{O}_{LR}^{\Delta B=2}\rangle&=M_{B_s}^2f_{B_s}^2\left[\frac{2M_{B_s}^2}{(\bar{m}_b(\mu_b)+\bar{m}_s(\mu_b))^2}+\frac{1}{3}\right]B_4(\mu_b).
\end{aligned}$$

The observable ΔM_s is calculated according to

$$\Delta M_s=2|M_{12}^s|, \tag{4.5}$$

where

$$\begin{aligned}
M_{12}^s=&\frac{G_F^2}{12\pi^2}\lambda_t^2M_W^2S_0(x_t)\hat{\eta}_Bf_{B_s}^2M_{B_s}B_1\\
&+\frac{1}{2M_{B_s}}[2C_{RR}^{\Delta B=2}\langle\mathcal{O}_{RR}^{\Delta B=2}\rangle+C_{LR}^{\Delta B=2}\langle\mathcal{O}_{LR}^{\Delta B=2}\rangle].
\end{aligned} \tag{4.6}$$

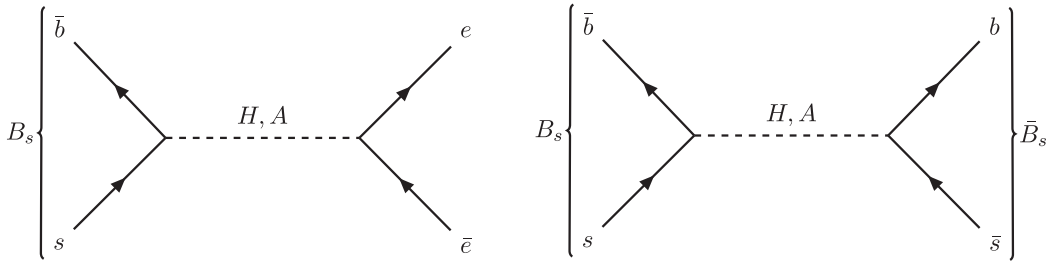

FIG. 2. Feynman diagrams for $B_s\to e^-e^+$ and $B_s-\overline{B}_s$ mixing induced at tree level by the scalar H and pseudoscalar A, respectively.

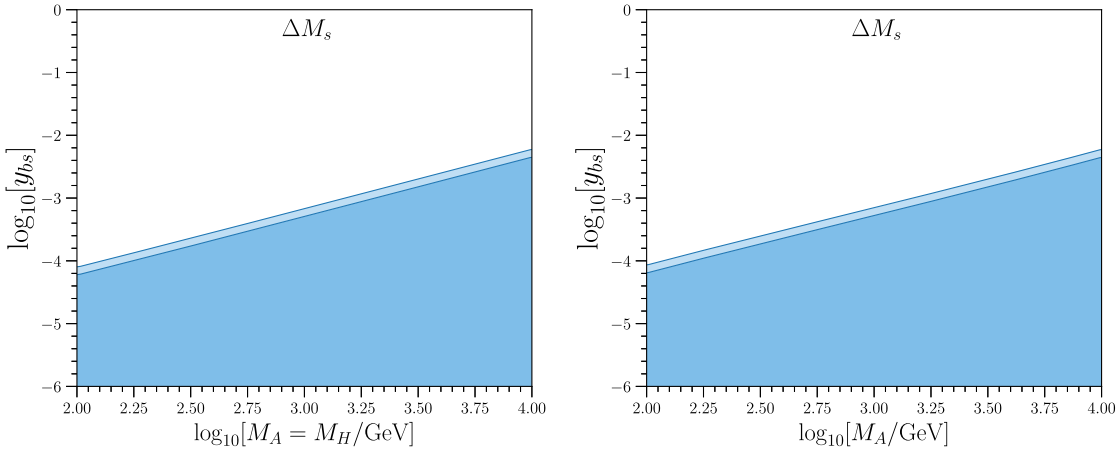

FIG. 3. Allowed parameter space of the quark coupling y_{bs} and new neutral Higgs mass M_A, from the measurement of mass mixing in the B_s system, ΔM_s. Left: in the limit of $M_A = M_H$. Right: we allow M_A and M_H to differ within the theoretical constraints of the model and minimize through M_H. In both plots, the contours in dark and light blue represent the allowed space within 1σ and 2σ, respectively.

To estimate ΔM_s we use FLAVIO. Our inputs are the Bag parameters given in [36] and the values for $|V_{us}|, |V_{cb}|, |V_{ub}|, \gamma$ from the CKMfitter's Spring 2021 update [37]. Thus, our determination in the SM is

$$\Delta M_s^{\text{SM}} = 17.49 \pm 0.64 \text{ ps}^{-1}. \tag{4.7}$$

This result agrees with previous calculations, but its central value is noticeably lower in comparison; consider for instance the result reported in [36] that reads $\Delta M_s^{\text{SM}} = 18.4^{+0.7}_{-1.2}$ ps^{-1}. This deviation is induced mainly by the update on the CKM inputs, more specifically by the $\sim 1\sigma$ decrease in $|V_{cb}|$ between the results from the CKMfitter's Summer 2018 report and the one from Spring 2021 [37]. The experimental result for ΔM_s is taken from [38]

$$\Delta M_s^{\text{Exp}} = 17.765 \pm 0.006 \text{ ps}^{-1}. \tag{4.8}$$

In Fig. 3, we present the constraint from the measured value of neutral B_s meson mixing, ΔM_s, for the allowed parameter space in the M_H vs y_{bs} plane, both in the limit of $M_A = M_H$ and allowing the maximum freedom between M_A and M_H from theory; the difference between these two scenarios is found to be minimal. This plot shows that in order to be in agreement with the measured value of ΔM_s, the coupling y_{bs} has to be small; e.g., for a mass of $M_A = 1$ TeV we find that $y_{bs} \lesssim 0.001$ at 2σ.

Furthermore, we can use the processes $B \to K^{(*)}e^+e^-$ to constrain simultaneously the couplings y_{bs} and y_{ee}. As a matter of fact, the NP effects in the transitions $B \to K^{(*)}e^+e^-$ can be parametrized directly in terms of the Wilson coefficients $C^{ee}_{S^{(\prime)}}$, $C^{ee}_{P^{(\prime)}}$ in Eq. (3.12) which also affect $B_s \to e^+e^-$. The $B \to K^{(*)}e^+e^-$ observables considered in this work are listed in Table I. Since the associated expressions for the observables in Table I are quite lengthy, we refer the interested reader to the FLAVIO's documentation and code [29]. Here we only quote explicitly the NP components of the helicity amplitudes for a pseudoscalar K or vector K^* final state kaon that depend on the Wilson coefficients $C^{ee}_{P^{(\prime)}}$ and $C^{ee}_{S^{(\prime)}}$

TABLE I. List of $B \to Ke^+e^-$ observables used to constrain the couplings y_{bs} and y_{ee} and the masses M_H and M_A. For P'_4 and P'_5, we consider the average of the B^+ and B^0 modes.

Observable	q^2 bin (GeV^2)	Exp. Avg.	SM Pred.
$10^8 \times \frac{\Delta\mathcal{B}}{\Delta q^2}(B^+ \to K^+e^+e^-)$	[1.0,6.0]	3.24 ± 0.65 [43,44]	3.37 ± 0.56
	[0.1,4.0]	4.70 ± 1.01 [44]	3.40 ± 0.58
	[4.0,8.12]	2.36 ± 0.79 [44]	3.31 ± 0.54
$10^7 \times \frac{\Delta\mathcal{B}}{\Delta q^2}(B^0 \to K^{*0}e^+e^-)$	[0.003,1.0]	3.09 ± 0.99 [45]	2.10 ± 0.35
$P'_4(B \to K^*e^+e^-)$	[1.0,6.0]	-0.71 ± 0.40 [46]	-0.34 ± 0.04
	[14.18,19.0]	-0.15 ± 0.41 [46]	-0.63 ± 0.01
$P'_5(B \to K^*e^+e^-)$	[1.0,6.0]	-0.23 ± 0.41 [46]	-0.42 ± 0.09
	[14.18,19.0]	-0.86 ± 0.34 [46]	-0.63 ± 0.03

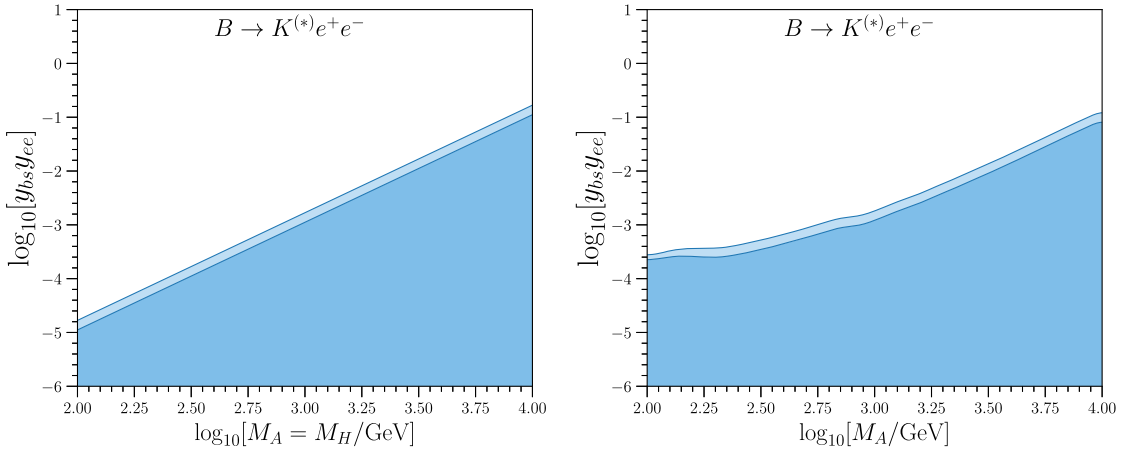

FIG. 4. Allowed parameter space for the coupling product $y_{bs}y_{ee}$ and the new neutral Higgs mass M_A, from the measurements of the $B \to K^{(*)}e^+e^-$ observables in Table I. Left: in the limit of $M_A = M_H$. Right: we allow M_A and M_H to differ within the theoretical constraints of the model and minimize through M_H. In both plots, the contours in dark and light blue represent the possible space within 1σ and 2σ, respectively.

$$h_S^{K^*} = \frac{i\lambda(m_B^2, m_{K^*}^2, q^2)}{2}(C_S^{ee} - C_{S'}^{ee})A_0(q^2), \quad (4.9)$$

$$h_P^{K^*} = \frac{i\lambda(m_B^2, m_{K^*}^2, q^2)}{2}(C_P^{ee} - C_{P'}^{ee} + \ldots)A_0(q^2), \quad (4.10)$$

$$h_S^{K} = \frac{m_B^2 - m_K^2}{2}(C_S^{ee} + C_{S'}^{ee})f_0(q^2), \quad (4.11)$$

$$h_P^{K} = \frac{m_B^2 - m_K^2}{2}(C_P^{ee} + C_{P'}^{ee} + \ldots)f_0(q^2), \quad (4.12)$$

where the ellipses stand for extra contributions including the purely SM ones in $C_{10^{(\prime)}}^{ee}$. Moreover, $\lambda(a,b,c)$ is the Källen function, and $A_0(q^2), f_0(q^2)$ are each one of the $B \to K^*$ and $B \to K$ form factors, respectively, which depend on the invariant dilepton mass squared q^2 and are constructed using [39–42]. In Eqs. (4.9) and (4.10) we can see that the NP contributions enter in terms of the differences of $\Delta C_S^{ee} = C_S^{ee} - C_{S'}^{ee}$ and $\Delta C_P^{ee} = C_P^{ee} - C_{P'}^{ee}$ as is the case for $B_s \to e^+e^-$ and therefore the $B \to K^*$ modes will only be sensitive to M_A. Conversely, from Eqs. (4.11) and (4.12), instead of the differences, the NP effects enter in terms of the sum of the relevant Wilson coefficients and so the $B \to K$ modes depend only on M_H.

In Fig. 4, we show the constraints arising from the combined fit of the $B \to K^{(*)}$ observables listed in Table I, both in the limit of $M_A = M_H$ and allowing the maximum freedom between M_A and M_H from theory. We can see that the product of the couplings $y_{bs}y_{ee}$ is expected to be small and is correlated with M_A and M_H similarly to the results drawn from ΔM_s for y_{bs}.

In Fig. 5 we present the allowed parameter space in the $y_{bs}y_{ee} - M_A$ plane from all constraints considered, where once more, we take into account two cases: first the limit $M_A = M_H$ and second the situation where the maximum freedom between M_A and M_H is allowed from theory. The region shaded in green is allowed by the LEP and the ΔM_s bounds. The region shaded in blue is allowed by the bound from the $B \to K^{(*)}e^+e^-$ processes. The black lines correspond to contours for constant values of the ratio $\bar{\mathcal{B}}r(B_s \to e^+e^-)/\bar{\mathcal{B}}r(B_s \to e^+e^-)_{\mathrm{SM}}$ that determine the enhancement in $\bar{\mathcal{B}}r(B_s \to e^+e^-)$ with respect to the SM prediction. Here we can see how an enhancement by a factor as large as 10^8 is allowed by the collider and B physics constraints. In fact, we can saturate the bound imposed by the LHCb analysis of $B_s \to e^+e^-$ reported in [11], which is shown by the red dashed line and requires an enhancement by a factor of 10^5.

Thus Fig. 5 contains one of the main results of this work: within the context of a type-III 2HDM, an enhancement on $\bar{\mathcal{B}}r(B_s \to e^+e^-)$ up to values that saturate the current experimental bounds is completely allowed and consistent with the different phenomenological constraints known from B physics and collider studies. Notice that in this section we have focused on determining the possible values that the coupling constants and masses of the type-III 2HDM affecting directly $B_s \to e^+e^-$ can assume, although so far we have not discussed how a model with such properties could arise from a UV-complete theory. This is precisely the task we undertake in the next section.

V. 2HDM AND QUARK-LEPTON UNIFICATION

In this section, we demonstrate how the coupling structure we have considered for the 2HDM can be obtained from a UV theory of quark-lepton unification that can live at a low energy scale. We focus on the NP

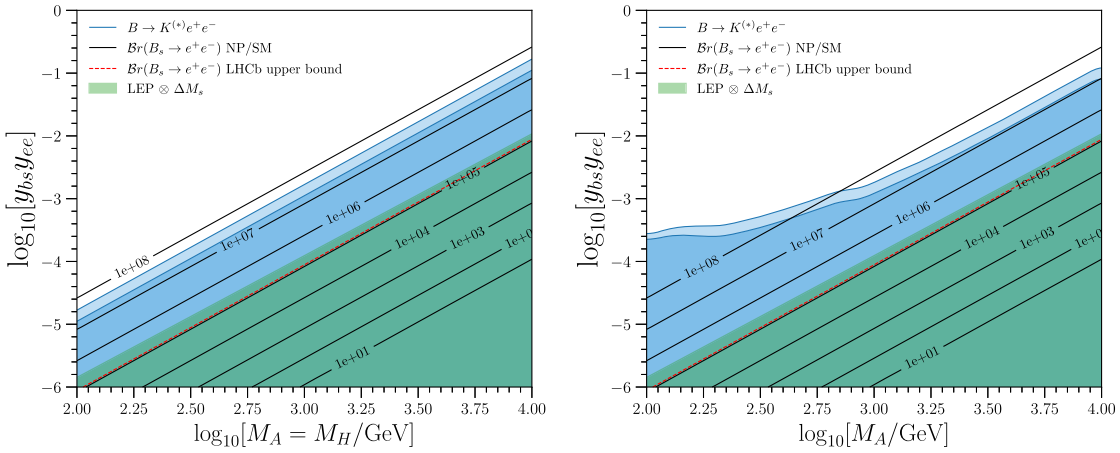

FIG. 5. Allowed parameter space for the coupling product $y_{bs}y_{ee}$ and the mass of the new neutral Higgs mass M_A. Left: in the limit of $M_A = M_H$. Right: we allow M_A and M_H to differ within the theoretical constraints of the model and minimize through M_H. In both plots, the contours in dark and light blue represent the possible space within 1σ and 2σ, respectively. The black lines correspond to contours for the ratio $\bar{\mathcal{B}}r(B_s \to e^+e^-)/\bar{\mathcal{B}}r(B_s \to e^+e^-)_{\mathrm{SM}}$. Notice that to saturate the current experimental bound it is required an enhancement of 10^5.

framework proposed in Ref. [20], which is based on the gauge group

$$\mathrm{SU}(4)_C \otimes \mathrm{SU}(2)_L \otimes \mathrm{U}(1)_R.$$

Moreover, it implements the inverse seesaw mechanism in order to generate neutrino masses and can be seen as a low energy limit of the Pati-Salam theory [15]. The phenomenology of the leptoquarks in this NP framework has been studied in [47,48], while the phenomenology of its scalar sector, which corresponds to a special case of the type-III 2HDM, has been recently analyzed in [49]. For further details we refer the reader to those references.

Within our framework, the SM matter fields are unified in the following representations:

$$F_{QL} = \begin{pmatrix} u_r & u_g & u_b & \nu \\ d_r & d_g & d_b & e \end{pmatrix} \sim (\mathbf{4}, \mathbf{2}, 0), \tag{5.1}$$

$$F_u = \begin{pmatrix} u_r^c & u_g^c & u_b^c & \nu^c \end{pmatrix} \sim (\bar{\mathbf{4}}, \mathbf{1}, -1/2), \tag{5.2}$$

$$F_d = \begin{pmatrix} d_r^c & d_g^c & d_b^c & e^c \end{pmatrix} \sim (\bar{\mathbf{4}}, \mathbf{1}, 1/2), \tag{5.3}$$

and hence, the leptons can be interpreted as the fourth color of the fermions. The Yukawa interactions for the charged fermions can be written as

$$-\mathcal{L}_Y \supset Y_1 F_{QL} F_u H_1 + Y_2 F_{QL} F_u \Phi + Y_3 H_1^\dagger F_{QL} F_d + Y_4 \Phi^\dagger F_{QL} F_d + \mathrm{H.c.}, \tag{5.4}$$

where $H_1 \sim (\mathbf{1}, \mathbf{2}, 1/2)$ and $\Phi \sim (\mathbf{15}, \mathbf{2}, 1/2)$ are required to generate fermion masses in a consistent manner. The Φ field contains a second Higgs doublet H_2 that is coupled to all the SM fermions

$$\Phi = \begin{pmatrix} \Phi_8 & \Phi_3 \\ \Phi_4 & 0 \end{pmatrix} + \sqrt{2} T_4 H_2 \sim (\mathbf{15}, \mathbf{2}, 1/2), \tag{5.5}$$

where T_4 is one of the generators of $\mathrm{SU}(4)_C$ and it is normalized as $T_4 = \frac{1}{2\sqrt{6}}\mathrm{diag}(1, 1, 1, -3)$.

Since the NP framework under consideration arises from quark-lepton unification there are only four independent Yukawa couplings (instead of eight) defining the interactions between the Higgs doublets and the SM fermions:

$$\begin{aligned} -\mathcal{L} = {} & \bar{u}_R \left(Y_1^T \tilde{H}_1 + \frac{1}{2\sqrt{3}} Y_2^T \tilde{H}_2 \right) Q_L \\ & + \bar{N}_R \left(Y_1^T \tilde{H}_1 - \frac{\sqrt{3}}{2} Y_2^T \tilde{H}_2 \right) \ell_L \\ & + \bar{d}_R \left(Y_3^T H_1^\dagger + \frac{1}{2\sqrt{3}} Y_4^T H_2^\dagger \right) Q_L \\ & + \bar{e}_R \left(Y_3^T H_1^\dagger - \frac{\sqrt{3}}{2} Y_4^T H_2^\dagger \right) \ell_L + \mathrm{H.c.}, \end{aligned} \tag{5.6}$$

and the VEVs are defined by $\langle H_1^0 \rangle = v_1/\sqrt{2}$ and $\langle H_2^0 \rangle = v_2/\sqrt{2}$.

As it was shown in Ref. [49], the interactions between the physical Higgs bosons and the SM down-type quarks and charged leptons are given, respectively, by

$$\tilde{Y}^\ell = (\tan\beta - 3\cot\beta)\frac{M^E_{\mathrm{diag}}}{4v} + 3(\tan\beta + \cot\beta)\frac{V_c^T M^D_{\mathrm{diag}} V}{4v}, \tag{5.7}$$

$$\tilde{Y}^d = (3\tan\beta - \cot\beta)\frac{M^D_{\rm diag}}{4v} + (\tan\beta + \cot\beta)\frac{V_c^* M^E_{\rm diag} V^\dagger}{4v}, \tag{5.8}$$

where V and V_c are unitary matrices that contain information about the unknown mixing between quarks and leptons. In addition, $M^D_{\rm diag}$ and $M^E_{\rm diag}$ are the diagonal mass matrices for down-type quarks and charged leptons. From Eqs. (5.7) and (5.8) above we can see that the theory predicts a correlation between the couplings to quarks and leptons. As it was demonstrated in Ref. [50], in the regimes with $\tan\beta \gg 1$ or $\tan\beta \ll 1$ the theory predicts unique relations among the decay widths of heavy Higgs bosons that can be probed at the LHC. Consequently, we focus on these two limits.

If we assume the complex phases to vanish, then the 3×3 unitary matrix V can be parametrized in terms of three mixing angles, which here we denote as θ_{12}, θ_{13}, and θ_{23}, as follows:

$$V = \begin{pmatrix} c_{12}c_{13} & s_{12}c_{13} & s_{13} \\ -s_{12}c_{23} - c_{12}s_{23}s_{13} & c_{12}c_{23} - s_{12}s_{23}s_{13} & s_{23}c_{13} \\ s_{12}s_{23} - c_{12}c_{23}s_{13} & -c_{12}s_{23} - s_{12}c_{23}s_{13} & c_{23}c_{13} \end{pmatrix}, \tag{5.9}$$

where we have used s_{ij} and c_{ij} as short notation for $\sin\theta_{ij}$ and $\cos\theta_{ij}$, respectively. An analogous expression can then also be written for V_c but with primed mixing angles s'_{ij} and c'_{ij}. For large $\tan\beta$ and in the limit where $s_{ij} \to 1$ and $s'_{ij} \to 1$ the interactions with the charged leptons are simplified to

$$\tilde{Y}^\ell = \frac{\tan\beta}{4v}\begin{pmatrix} m_e + 3m_b & \varepsilon & \varepsilon \\ \varepsilon & m_\mu + 3m_s & \varepsilon \\ \varepsilon & \varepsilon & m_\tau + 3m_d \end{pmatrix}, \tag{5.10}$$

which gives us the flavor-diagonal couplings with the hierarchy $y_{ee} \gg y_{\mu\mu}, y_{\tau\tau}$. This motivates our choice for the couplings in Sec. III. The same conclusions hold for intermediate and small values of $\tan\beta$.

For the down-type quarks and large $\tan\beta$, we get the following interaction matrix

$$\tilde{Y}^d = \frac{\tan\beta}{4v}\begin{pmatrix} 3m_d + m_\tau & \varepsilon & \varepsilon \\ \varepsilon & 3m_s + m_\mu & \varepsilon \\ \varepsilon & \varepsilon & 3m_b + m_e \end{pmatrix}, \tag{5.11}$$

which gives us the hierarchy $y_{dd} \simeq y_{bb} \gg y_{ss}$. The same conclusion holds for intermediate and small values of $\tan\beta$.

Unfortunately, due to the freedom in the coupling to the right-handed neutrinos, the theory does not predict the coupling of the Higgs bosons to the up-type quarks.

Since we require a nonzero y_{bs} coupling, we set all $s_{ij} = s'_{ij} = 1$ except for s_{23} and s'_{23}; this choice is motivated by requiring the first-generation off-diagonal couplings to be vanishing. From quark-lepton unification, nonzero entries for $\tilde{Y}^d_{bs}$ and $\tilde{Y}^d_{sb}$ imply nonzero values for $\tilde{Y}^\ell_{\mu\tau}$ and $\tilde{Y}^\ell_{\tau\mu}$. Namely,

$$\tilde{Y}^d_{sb} = \frac{1}{4v}(\tan\beta + \cot\beta)(m_\mu s'_{23}c_{23} - m_e s_{23}c'_{23}), \tag{5.12}$$

$$\tilde{Y}^d_{bs} = \frac{1}{4v}(\tan\beta + \cot\beta)(m_\mu s_{23}c'_{23} - m_e s'_{23}c_{23}), \tag{5.13}$$

$$\tilde{Y}^\ell_{\mu\tau} = \frac{3}{4v}(\tan\beta + \cot\beta)(m_s s'_{23}c_{23} - m_d s_{23}c'_{23}), \tag{5.14}$$

$$\tilde{Y}^\ell_{\tau\mu} = \frac{3}{4v}(\tan\beta + \cot\beta)(m_s s_{23}c'_{23} - m_d s'_{23}c_{23}), \tag{5.15}$$

whenever $s_{23} = s'_{23}$ then we have that $\tilde{Y}^d_{sb} = \tilde{Y}^d_{bs} = y_{bs}/2$, which motivates the choice made in Eq. (3.9); we also have that $\tilde{Y}^\ell_{\mu\tau} = \tilde{Y}^\ell_{\tau\mu} = y_{\tau\mu}/2$. The $\tau\mu$ couplings will generate the following dimension-six operators

$$\begin{aligned}\mathcal{H}_{\rm eff} \supset & -\frac{y_{ee}y_{\mu\tau}}{M_H^2}(\bar{\tau}\mu)(\bar{e}e) - \frac{y_{\tau\tau}y_{\mu\tau}}{M_H^2}(\bar{\tau}\mu)(\bar{\tau}\tau) \\ & + \frac{y_{ee}y_{\mu\tau}}{M_A^2}(\bar{\tau}\gamma^5\mu)(\bar{e}\gamma^5 e) + \frac{y_{\tau\tau}y_{\mu\tau}}{M_A^2}(\bar{\tau}\gamma^5\mu)(\bar{\tau}\gamma^5\tau),\end{aligned} \tag{5.16}$$

which will induce the lepton-flavor-violating decay $\tau^\pm \to \mu^\pm e^- e^+$ at tree level, and $\tau^\pm \to \mu^\pm\gamma$ at one loop. The current experimental bounds on these decay channels are $\mathcal{B}r(\tau \to \mu\gamma) < 4.4\times 10^{-8}$ [51] and $\mathcal{B}r(\tau^- \to \mu^- e^+ e^-) < 1.8\times 10^{-8}$ [52]. These bounds are expected to be improved by future B factories [53].

The effective operators $\{(\bar{\tau}\mu)(\bar{e}e), (\bar{\tau}\gamma^5\mu)(\bar{e}\gamma^5 e)\}$ in Eq. (5.16) can be mapped to operators that are analogous to $\mathcal{O}^{\Delta B=2}_{LL}$, $\mathcal{O}^{\Delta B=2}_{RR}$, and $\mathcal{O}^{\Delta B=2}_{LR}$ in Eq. (4.3), and hence, the corresponding Wilson coefficients have also analogous expressions to the coefficients shown in Eq. (4.4). More precisely, the new set of operators to be considered is

$$\begin{aligned}\mathcal{O}^{ee}_{LL} &= \bar{\tau}(1-\gamma_5)\mu\bar{e}(1-\gamma_5)e, \\ \mathcal{O}^{ee}_{RR} &= \bar{\tau}(1+\gamma_5)\mu\bar{e}(1+\gamma_5)e, \\ \mathcal{O}^{ee}_{LR} &= \bar{\tau}(1-\gamma_5)\mu\bar{e}(1+\gamma_5)e, \\ \mathcal{O}^{ee}_{RL} &= \bar{\tau}(1+\gamma_5)\mu\bar{e}(1-\gamma_5)e,\end{aligned} \tag{5.17}$$

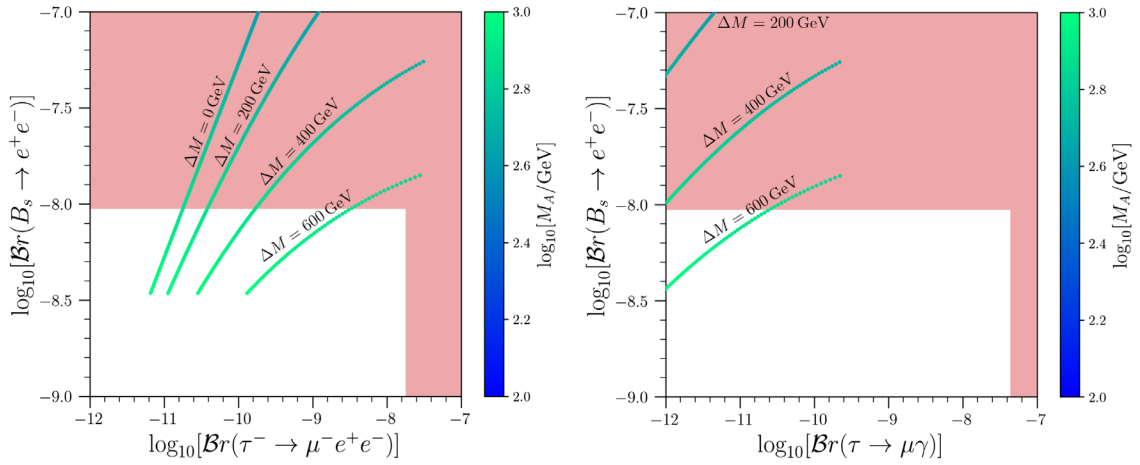

FIG. 6. Left: predicted correlation between $\bar{\mathcal{B}}r(B_s \to e^+e^-)$ and $\mathcal{B}r(\tau^- \to \mu^-e^+e^-)$. The regions shaded in red correspond to the experimental bounds for each decay, respectively. The different bands correspond to different values for the mass splitting $\Delta M \equiv M_A - M_H$. We have fixed $s_{23} = s'_{23} = 0.98$ and $\tan\beta = 10$. Right: same as the left panel for the predicted correlation between $\bar{\mathcal{B}}r(B_s \to e^+e^-)$ and $\mathcal{B}r(\tau \to \mu\gamma)$.

with coefficients

$$C^{ee}_{LL} = C^{ee}_{RR} = \frac{y_{ee}y_{\mu\tau}}{4}\left[\frac{1}{M_H^2} - \frac{1}{M_A^2}\right],$$
$$C^{ee}_{LR} = C^{ee}_{RL} = \frac{y_{ee}y_{\mu\tau}}{4}\left[\frac{1}{M_H^2} + \frac{1}{M_A^2}\right]. \tag{5.18}$$

Similar expressions follow for operators constructed from the set $\{(\bar{\tau}\mu)(\tau\bar{\tau}), (\bar{\tau}\gamma^5\mu)(\tau\gamma^5\bar{\tau})\}$ with corresponding Wilson coefficients $C^{\tau\tau}_{LL}, C^{\tau\tau}_{RR}, C^{\tau\tau}_{LR}$, and $C^{\tau\tau}_{RL}$. After implementing these effective operators, we proceed to compute the τ decays in FLAVIO. In order to obtain a large contribution to $\tau \to \mu\gamma$, we require that $C^{\tau\tau}_{RR}$ and $C^{\tau\tau}_{LL}$ be nonzero, and hence a mass splitting between H and A is needed.

Our theoretical setup has effects on the decay channel $B_s \to \mu^+\mu^-$, which depends on the Wilson coefficients $C^{\mu\mu}_S$ and $C^{\mu\mu}_P$, which are analogous to C^{ee}_S and C^{ee}_P for $B_s \to e^+e^-$ with the leptonic coupling y_{ee} replaced by $y_{\mu\mu}$, see Eq. (3.11). Since we have $y_{\mu\mu} \ll y_{ee}$ this implies that the NP contribution will be much smaller for muons than for electrons. Nonetheless, we have checked that for each point in the allowed parameter space the prediction for $\bar{\mathcal{B}}r(B_s \to \mu^+\mu^-)$ is in agreement with the experimental measurement given in Eq. (2.17) within 2σ.

Now, let us analyze the effects on $\bar{\mathcal{B}}r(B_s \to e^+e^-)$ and the lepton-flavor-violating decays. First, we provide a concrete example on how large the enhancement in $\mathcal{B}r(B_s \to e^+e^-)$ can be within the theory under consideration for concrete values of the input parameters. Thus, we fix the mass of the scalar and pseudoscalar to $M_A = 800$ GeV, $M_H = 400$ GeV and the rest of the parameters to $\tan\beta = 10$ and $s_{23} = s'_{23} = 0.98$. This implies an electron coupling of $y_{ee} \simeq 0.13$, which is in agreement with the bound from LEP. For the off-diagonal quark coupling we obtain $y_{bs} \simeq 4.2 \times 10^{-4}$, which gives $\bar{\mathcal{B}}r(B_s \to e^+e^-) \simeq 8.4 \times 10^{-9}$. For the choice of mixing angles discussed above, the off-diagonal lepton coupling is $y_{\tau\mu} \simeq 1.1 \times 10^{-3}$ and predicts $\mathcal{B}r(\tau^- \to \mu^-e^+e^-) \simeq 1.4 \times 10^{-10}$ and $\mathcal{B}r(\tau \to \mu\gamma) \simeq 6.6 \times 10^{-13}$.

Finally, we can generalize the previous exercise while at the same time assessing the impact on lepton-flavor-violating decays. Then, in the left panel of Fig. 6 we show the predicted correlation between the observables $\bar{\mathcal{B}}r(B_s \to e^+e^-)$ and $\bar{\mathcal{B}}r(\tau^- \to \mu^-e^+e^-)$. The different bands correspond to different values for the mass splitting $\Delta M \equiv M_A - M_H$. We fix $s_{23} = s'_{23} = 0.98$ and $\tan\beta = 10$. The region shaded in red corresponds to the current experimental limits on these observables. In the right panel in Fig. 6 we show the correlation between $\bar{\mathcal{B}}r(B_s \to e^+e^-)$ and $\mathcal{B}r(\tau \to \mu\gamma)$. From Fig. 6 we can see that it is possible to saturate the current experimental bounds in $\bar{\mathcal{B}}r(B_s \to e^+e^-)$ while at the same time obeying the constraints on the lepton-flavor-violating decays. This is the second result that we want to highlight in this work. These plots provide a set of correlations between different channels which make this framework phenomenologically testable.

VI. SUMMARY

The leptonic decay $B_s \to e^+e^-$ is a decay channel with interesting properties and it can be used as smoking gun in the search for new physics. For instance, it is exceptionally clean. Moreover if this process takes place as predicted by the Standard Model, due to the helicity suppression effect, its tiny decay probability places it outside the reach of current or forthcoming particle physics experiments. Therefore, any observation of this channel in the near future

would represent conclusive evidence for physics beyond the Standard Model.

In this article and to the best of our knowledge, we have presented for the first time, a concrete new physics scenario that can provide a large enhancement on the decay width for the channel $B_s \to e^+e^-$. More specifically, by studying the general 2HDM in which both doublets are coupled to the quarks and leptons of the Standard Model, we have demonstrated that when the CP-odd scalar A is mostly coupled to electrons, it can give a contribution to the transition $B_s \to e^+e^-$, which enhances its decay probability by up to five orders of magnitude above the Standard Model prediction, saturating the most recent experimental upper bound established by the LHCb collaboration. We have identified regions in the corresponding parameter space where this potential enhancement respects all known constraints from flavor and collider physics, including for instance neutral B_s mixing as well as LEP measurements of the $e^-e^+ \to e^-e^+$ cross section.

Furthermore, we have shown how the required coupling structure for the 2HDM can arise from a UV theory of quark-lepton unification that can be realized at a low energy scale. This framework predicts a correlation between the decay channel $B_s \to e^+e^-$ and the lepton-flavor-violating decays $\tau^- \to \mu^-e^+e^-$ and $\tau \to \mu\gamma$. We have worked out quantitatively the interplay between these channels for different values of the relevant free parameters. If the decay process $B_s \to e^+e^-$ is observed in the near future, then the presence of heavy (pseudo)scalars can be further confirmed by searches for a heavy resonance decaying into an electron-positron pair at the LHC. Our results show that the channel $B_s \to e^+e^-$ is indeed a very interesting candidate to probe for new physics effects and provides additional justification to pursue further experimental searches for it in the current and foreseeable experiments.

ACKNOWLEDGMENTS

This project has received funding from the European Union's Horizon 2020 research and innovation programme under the Marie Skłodowska-Curie Grant Agreement No. 945422. A. D. P. is supported by the INFN "Iniziativa Specifica" Theoretical Astroparticle Physics (TAsP-LNF) and by the Frascati National Laboratories (LNF) through a Cabibbo Fellowship, call 2020. M. B. and G. T-X. are supported by Deutsche Forschungsgemeinschaft (DFG, German Research Foundation) through Grant No. 396021762-TRR 257 "Particle Physics Phenomenology after the Higgs Discovery." Parts of the computations carried out for this work made use of the OMNI cluster of the University of Siegen. We acknowledge useful communication with Alexander Lenz and Matthew Kirk on the current updates of $B_s \to \mu^+\mu-$.

[1] Y. Aoki *et al.*, FLAG review 2021, Eur. Phys. J. C **82**, 869 (2022).
[2] A. Bazavov *et al.*, B- and D-meson leptonic decay constants from four-flavor lattice QCD, Phys. Rev. D **98**, 074512 (2018).
[3] A. Bussone *et al.* (ETM Collaboration), Mass of the b quark and B-meson decay constants from $N_f = 2 + 1 + 1$ twisted-mass lattice QCD, Phys. Rev. D **93**, 114505 (2016).
[4] R. J. Dowdall, C. T. H. Davies, R. R. Horgan, C. J. Monahan, and J. Shigemitsu (HPQCD Collaboration), B-Meson Decay Constants from Improved Lattice Nonrelativistic QCD with Physical u, d, s, and c Quarks, Phys. Rev. Lett. **110**, 222003 (2013).
[5] C. Hughes, C. T. H. Davies, and C. J. Monahan, New methods for B meson decay constants and form factors from lattice NRQCD, Phys. Rev. D **97**, 054509 (2018).
[6] R. Aaij *et al.* (LHCb Collaboration), Measurement of the $B_s^0 \to \mu^+\mu^-$ decay properties and search for the $B^0 \to \mu^+\mu^-$ and $B_s^0 \to \mu^+\mu^-\gamma$ decays, Phys. Rev. D **105**, 012010 (2022).
[7] R. Aaij *et al.* (LHCb Collaboration), Analysis of Neutral B-Meson Decays into Two Muons, Phys. Rev. Lett. **128**, 041801 (2022).
[8] M. Aaboud *et al.* (ATLAS Collaboration), Study of the rare decays of B_s^0 and B^0 mesons into muon pairs using data collected during 2015 and 2016 with the ATLAS detector, J. High Energy Phys. 04 (2019) 098.
[9] CMS Collaboration, Measurement of $B_s^0 \to \mu^+\mu^-$ decay properties and search for the $B^0 \to \mu\mu$ decay in proton-proton collisions at $\sqrt{s} = 13$ TeV, Report No. CMS-PAS-BPH-21-006.
[10] T. Aaltonen *et al.* (CDF Collaboration), Search for the Decays $B_s^0 \to e^+\mu^-$ and $B_s^0 \to e^+e^-$ in CDF Run II, Phys. Rev. Lett. **102**, 201801 (2009).
[11] R. Aaij *et al.* (LHCb Collaboration), Search for the Rare Decays $B_s^0 \to e^+e^-$ and $B^0 \to e^+e^-$, Phys. Rev. Lett. **124**, 211802 (2020).
[12] R. Fleischer, R. Jaarsma, and G. Tetlalmatzi-Xolocotzi, In pursuit of new physics with $B_{s,d}^0 \to \ell^+\ell^-$, J. High Energy Phys. 05 (2017) 156.
[13] J. F. Gunion, H. E. Haber, G. L. Kane, and S. Dawson, *The Higgs Hunter's Guide* (CRC Press, Boca Raton, 1990).
[14] G. C. Branco, P. M. Ferreira, L. Lavoura, M. N. Rebelo, M. Sher, and J. P. Silva, Theory and phenomenology of two-Higgs-doublet models, Phys. Rep. **516**, 1 (2012).
[15] J. C. Pati and A. Salam, Lepton number as the fourth color, Phys. Rev. D **10**, 275 (1974).
[16] P. Minkowski, $\mu \to e\gamma$ at a rate of one out of 10^9 muon decays?, Phys. Lett. **67B**, 421 (1977).

[17] T. Yanagida, Horizontal gauge symmetry and masses of neutrinos, Conf. Proc. C **7902131**, 95 (1979).

[18] M. Gell-Mann, P. Ramond, and R. Slansky, Complex spinors and unified theories, Conf. Proc. C **790927**, 315 (1979).

[19] R. N. Mohapatra and G. Senjanovic, Neutrino Mass and Spontaneous Parity Nonconservation, Phys. Rev. Lett. **44**, 912 (1980).

[20] P. Fileviez Perez and M. B. Wise, Low scale quark-lepton unification, Phys. Rev. D **88**, 057703 (2013).

[21] R. N. Mohapatra, Mechanism for Understanding Small Neutrino Mass in Superstring Theories, Phys. Rev. Lett. **56**, 561 (1986).

[22] R. N. Mohapatra and J. W. F. Valle, Neutrino mass and baryon number nonconservation in superstring models, Phys. Rev. D **34**, 1642 (1986).

[23] K. De Bruyn, R. Fleischer, R. Knegjens, P. Koppenburg, M. Merk, A. Pellegrino, and N. Tuning, Probing New Physics via the $B_s^0 \to \mu^+\mu^-$ Effective Lifetime, Phys. Rev. Lett. **109**, 041801 (2012).

[24] W. Altmannshofer and P. Stangl, New physics in rare B decays after Moriond 2021, Eur. Phys. J. C **81**, 952 (2021).

[25] R. Aaij *et al.* (LHCb Collaboration), Measurement of the $B_s^0 \to \mu^+\mu^-$ Branching Fraction and Effective Lifetime and Search for $B^0 \to \mu^+\mu^-$ Decays, Phys. Rev. Lett. **118**, 191801 (2017).

[26] A. Crivellin, A. Kokulu, and C. Greub, Flavor-phenomenology of two-Higgs-doublet models with generic Yukawa structure, Phys. Rev. D **87**, 094031 (2013).

[27] A. Crivellin, D. Müller, and C. Wiegand, $b \to s\ell^+\ell^-$ transitions in two-Higgs-doublet models, J. High Energy Phys. 06 (2019) 119.

[28] R. Aaij *et al.* (LHCb Collaboration), Search for the Decays $B_s^0 \to \tau^+\tau^-$ and $B^0 \to \tau^+\tau^-$, Phys. Rev. Lett. **118**, 251802 (2017).

[29] D. M. Straub, FLAVIO: A PYTHON package for flavour and precision phenomenology in the standard model and beyond, arXiv:1810.08132.

[30] A. M. Baldini *et al.* (MEG Collaboration), Search for the lepton flavour violating decay $\mu^+ \to e^+\gamma$ with the full dataset of the MEG experiment, Eur. Phys. J. C **76**, 434 (2016).

[31] W. H. Bertl *et al.* (SINDRUM II Collaboration), A search for muon to electron conversion in muonic gold, Eur. Phys. J. C **47**, 337 (2006).

[32] U. Bellgardt *et al.* (SINDRUM Collaboration), Search for the decay $\mu^+ \to e^+e^+e^-$, Nucl. Phys. **B299**, 1 (1988).

[33] J. F. Gunion and H. E. Haber, The *CP* conserving two Higgs doublet model: The approach to the decoupling limit, Phys. Rev. D **67**, 075019 (2003).

[34] R. L. Workman *et al.* (Particle Data Group), Review of particle physics, Prog. Theor. Exp. Phys. **2022**, 083C01 (2022).

[35] J. Alcaraz *et al.* (ALEPH, DELPHI, L3, OPAL, LEP Electroweak Working Group Collaborations), A Combination of preliminary electroweak measurements and constraints on the standard model, arXiv:hep-ex/0612034.

[36] L. Di Luzio, M. Kirk, A. Lenz, and T. Rauh, ΔM_s theory precision confronts flavour anomalies, J. High Energy Phys. 12 (2019) 009.

[37] J. Charles, A. Hocker, H. Lacker, S. Laplace, F. R. Le Diberder, J. Malcles *et al.* (CKMfitter Group), *CP* violation and the CKM matrix: Assessing the impact of the asymmetric *B* factories, Eur. Phys. J. C **41**, 1 (2005).

[38] Y. Amhis *et al.* (HFLAV Collaboration), Averages of *b*-hadron, *c*-hadron, and τ-lepton properties as of 2021, arXiv:2206.07501.

[39] J. A. Bailey *et al.*, $B \to Kl^+l^-$ decay form factors from three-flavor lattice QCD, Phys. Rev. D **93**, 025026 (2016).

[40] R. R. Horgan, Z. Liu, S. Meinel, and M. Wingate, Rare *B* decays using lattice QCD form factors, Proc. Sci., LATTICE2014 (**2015**) 372.

[41] A. Bharucha, D. M. Straub, and R. Zwicky, $B \to V\ell^+\ell^-$ in the standard model from light-cone sum rules, J. High Energy Phys. 08 (2016) 098.

[42] N. Gubernari, A. Kokulu, and D. van Dyk, $B \to P$ and $B \to V$ form factors from *B*-meson light-cone sum rules beyond leading twist, J. High Energy Phys. 01 (2019) 150.

[43] R. Aaij *et al.* (LHCb Collaboration), Test of Lepton Universality Using $B^+ \to K^+\ell^+\ell^-$ Decays, Phys. Rev. Lett. **113**, 151601 (2014).

[44] S. Choudhury *et al.* (BELLE Collaboration), Test of lepton flavor universality and search for lepton flavor violation in $B \to K\ell\ell$ decays, J. High Energy Phys. 03 (2021) 105.

[45] R. Aaij *et al.* (LHCb Collaboration), Measurement of the $B^0 \to K^{*0}e^+e^-$ branching fraction at low dilepton mass, J. High Energy Phys. 05 (2013) 159.

[46] S. Wehle *et al.* (Belle Collaboration), Lepton-Flavor-Dependent Angular Analysis of $B \to K^*\ell^+\ell^-$, Phys. Rev. Lett. **118**, 111801 (2017).

[47] P. Fileviez Perez, C. Murgui, and A. D. Plascencia, Leptoquarks and matter unification: Flavor anomalies and the muon g-2, Phys. Rev. D **104**, 035041 (2021).

[48] P. Fileviez Perez and C. Murgui, Flavor anomalies and quark-lepton unification, Phys. Rev. D **106**, 035033 (2022).

[49] P. Fileviez Perez, E. Golias, and A. D. Plascencia, Two-Higgs-doublet model and quark-lepton unification, J. High Energy Phys. 08 (2022) 293.

[50] P. Fileviez Perez, E. Golias, and A. D. Plascencia, Probing quark-lepton unification with leptoquark and Higgs boson decays, Phys. Rev. D **105**, 075011 (2022).

[51] B. Aubert *et al.* (*BABAR* Collaboration), Searches for Lepton Flavor Violation in the Decays $\tau^\pm \to e^\pm\gamma$ and $\tau^\pm \to \mu^\pm\gamma$, Phys. Rev. Lett. **104**, 021802 (2010).

[52] K. Hayasaka *et al.*, Search for lepton flavor violating τ decays into three leptons with 719 million produced $\tau^+\tau^-$ pairs, Phys. Lett. B **687**, 139 (2010).

[53] B. O'Leary *et al.* (SuperB Collaboration), SuperB progress reports—physics, arXiv:1008.1541.